HHS Public Access

Author manuscript

Nat Chem Biol. Author manuscript; available in PMC 2016 July 11.

Published in final edited form as:

Nat Chem Biol. 2016 March ; 12(3): 141–145. doi:10.1038/nchembio.1999.

Protonation of a Glutamate Residue Modulates the Dynamics of the Drug Transporter EmrE

Anindita Gayen[+], **Maureen Leninger**[+], and **Nathaniel J. Traaseth**[*]

Department of Chemistry, New York University, New York, NY 10003

Abstract

Secondary active transport proteins play a central role in conferring bacterial multidrug resistance. In this work, we investigated the proton-coupled transport mechanism for the *Escherichia coli* drug efflux pump EmrE using nuclear magnetic resonance (NMR) spectroscopy. Our results show that the global conformational motions necessary for transport are modulated in an allosteric fashion by the protonation state of a membrane-embedded glutamate residue. These observations directly correlate with the resistance phenotype for EmrE and the E14D mutant as a function of pH. Furthermore, our results support a model in which the pH gradient across the inner membrane of *E. coli* may be used on a mechanistic level to shift the equilibrium of the transporter in favor of an inward-open resting conformation poised for drug binding.

INTRODUCTION

Secondary active transporters provide a primary defense mechanism in conferring multidrug resistance (MDR) to bacteria. These integral membrane proteins bind and transport lethal compounds across the lipid bilayer and in the process reduce drug toxicity in the cytoplasm[1]. Antiporters from the small multidrug resistance (SMR) family represent an excellent system to study ion-coupled transport due to their small size (~100–120 residues) and importance in both antiseptic resistance[2] and membrane protein evolution[3]. EmrE is a member of this family that carries out drug efflux as a homodimer by coupling transport with the electrochemical potential across the inner membrane of *E. coli*[4]. The available structural models of EmrE depict an anti-parallel dimer arrangement[5–7] that stems from the dual topology insertion in the membrane[3]. While it is known that a conserved glutamate residue (Glu-14) within the first transmembrane (TM) domain of EmrE plays a central role in

[*]Corresponding author: ; Email: traaseth@nyu.edu. Department of Chemistry, New York University, 100 Washington Square East, New York, NY 10003

[+]These authors made an equal contribution to this work.

AUTHOR CONTRIBUTIONS

N.J.T. designed the project. A.G. and M.L. carried out the solution NMR, solid-state NMR, fluorescence experiments, and ethidium resistance assays. All authors analyzed the data. N.J.T. wrote the manuscript.

COMPETING FINANCIAL INTERESTS

The authors declare no competing financial interests.

ADDITIONAL INFORMATION

Supplementary information is available in the online version of the paper. Reprints and permissions information is available at www.nature.com/reprints/index.html. Correspondence and requests for materials should be addressed to N.J.T. (traaseth@nyu.edu).

transport[8], the mechanistic details concerning how this anionic residue couples efflux with the pH gradient have not been elucidated. In this work, we used a combination of drug resistance assays and biophysical experiments including solution and solid-state NMR spectroscopy to probe the conformational dynamics and allosteric communication within EmrE that underlie the ion-coupled mechanism.

RESULTS

pH Titration of EmrE Using Solution NMR Spectroscopy

Since previous work implicated a direct role for Glu-14 in drug efflux[8], we used solution NMR spectroscopy to measure the proton affinity with site-specific resolution. EmrE was isotopically enriched with ^{13}C at all Ile $C^{\delta 1}$ methyl groups and reconstituted into DMPC/DHPC isotropic bicelles as described previously[9]. The chemical shifts were recorded using $^{1}H/^{13}C$ heteronuclear correlation experiments and were assigned through a single-site mutagenesis method involving replacement of Ile residues to either Leu or Val (example spectra are shown in Supplementary Results, Supplementary Figure 1). Similar to our previous observations for drug-free EmrE[9,10], we observed systematic peak doubling for 14 out of the 15 Ile residues, which stems from the asymmetric nature of the dimer structure[6,7,11] (Figure 1a). The only exception was Ile-38 that likely had similar environments for both monomer subunits. Importantly, a spectral comparison of EmrE in DMPC and *E. coli* bicelles was remarkably similar in both the drug-free and drug-bound forms (Supplementary Figure 2), which supports the presence of a native fold under our experimental conditions.

To gauge the effect of acid/base chemistry on the transporter, the pH was varied from 5.0 to 9.15 with $^{1}H/^{13}C$ SOFAST HMQC[12] correlation spectra recorded at each value. In this titration, several significant chemical shift perturbations near and far from Glu-14 were detected suggesting that the acid/base chemistry had a pronounced effect on the structure of the transporter (Figure 1a). Since the pH may affect residues other than Glu-14, a control experiment was carried out using the E14Q mutant of EmrE, which was anticipated to behave like a fully protonated transporter at position 14. As seen in Supplementary Figure 3a, no significant perturbations were observed in the titration, which confirmed that the spectral changes for wild-type EmrE resulted from Glu-14 protonation/deprotonation. In addition, the E14Q spectrum was much more similar to the wild-type protein at low pH compared to high pH, which further shows that this mutant was a good mimic of the fully protonated transporter (Supplementary Figure 3b).

To quantify the pH-induced perturbations, the chemical shifts for wild-type EmrE were plotted against the pH. Most residues showed a classical two-state transition and thus the apparent acid dissociation constant for Glu-14 was obtained by fitting 18 ^{1}H and ^{13}C chemical shifts in a global fashion to a modified Henderson-Hasselbalch equation given in Eq. 1 of the Online Methods (average of the normalized shifts are shown in Figure 1b). The apparent pKa value of 7.0 ± 0.2 for the wild-type protein at 25 °C was in agreement with the estimated values reported from fluorescence measurements[13]. In addition, individual residues were fit to a single apparent pKa value with nearly all residues within the range of 6.8 to 7.2. It is important to note that our data cannot definitely rule out the possibility of

two pKa values for Glu-14. However, we emphasize that the single transition we report reflects the largest chemical shift changes observed in the titration (i.e., most significant structural change) and suggests that the two Glu-14 residues in the binding pocket have the same or similar pKa values within the experimental error of our measurements. This is also supported by individual fits for each monomer of EmrE, which resulted in apparent pKa values within 0.1 units of each other (Supplementary Figure 4). To further elucidate the mechanism of the native Glu-14 residue in EmrE, we carried out a similar pH titration with an E14D mutant that was previously shown to uncouple drug transport and confer limited drug resistance to *E. coli*[13]. Similar to E14Q, the Asp side chain of the mutant showed no major chemical shift changes over the pH range of 6.5 to 7.5, indicating an altered pKa for Asp-14 (Supplementary Figure 3a). Upon further reduction of pH, we observed spectral perturbations similar to the wild-type that enabled us to determine the more acidic apparent pKa value of 5.0 ± 0.2 (Figure 1c, d).

Ethidium Resistance Assays of EmrE and the E14D Mutant

With the apparent acid dissociation constant of the conserved anionic residue determined, we aimed to understand how these observables may affect the resistance phenotype of the E14D mutant and wild-type as a function of pH. Ethidium resistance assays were carried out with *E. coli* transformed with plasmids corresponding to wild-type EmrE, E14D, and a control vector at pH 7.0 and 4.7 using a 10-fold serial dilution assay to assess the phenotype conferred by the transporter. The results at neutral pH showed only wild-type EmrE to confer resistance (Figure 1e; growth up to 10^6 dilution) and are in agreement with previous findings that showed E14D to be essentially inactive under these conditions[14]. To the contrary, the resistance assays carried out at pH 4.7 indicated that E14D was able to confer a phenotype up to 10^4 dilution factor while the control only grew at a dilution of 10-fold (Figure 1e). Since this ~1000-fold difference was not observed at pH 7.0, these results support the conclusion that the pKa should be approximately between the pH of the cytoplasm (~7.6) and periplasm (same as external environment[15]) in order to confer catalytic competency for coupling drug efflux with proton transport. This conclusion is consistent with the competition model proposed for EmrE[4].

pH-Dependent Conformational Dynamics of EmrE

The alternating access model requires a transporter to exchange between at least two major conformations to carry out transport of drugs and protons (i.e., inward-open and outward-open; see model in Figure 2a)[16]. Due to the associated angular changes of the helices within the membrane, the oriented solid-state NMR approach is a sensitive method to capture these conformational changes in a direct fashion[17,18]. We previously showed that each monomer within the EmrE dimer possessed different helical tilt angles with respect to the bilayer surface[10] with the two peaks for each residue corresponding to the monomers within the asymmetric dimer[5,7]. Since these two populations interconverted on the msec-to-sec timescale[9] and the conformational dynamics of EmrE are necessary for ethidium efflux across membranes[19], these previous findings establish the ability to monitor exchange dynamics between inward-open and outward-open conformations using NMR spectroscopy in bicelles. To directly probe the exchange dynamics of EmrE as a function of pH, we utilized the PUREX method[20] in magnetically aligned lipid bicelles (DMPC/DHPC, 3.5/1),

which has been previously implemented in our laboratory[9]. Similar to the pH titration experiments, we recorded a series of PUREX datasets over a range of pH values (Supplementary Figure 5). The quantified exchange rates showed that the fastest conversion between inward-open and outward-open states occurred at acidic pH values while slower rates were observed at pH values above the apparent pKa for Glu-14 (Figure 2b, c). In support of these measurements, methyl T_{1zz} experiments were recorded at pH 9.15 (~2 units above the apparent pKa) using solution NMR and also showed intense exchange peaks between the two populations consistent with the PUREX results (Figure 2d). These data suggest an apparent two-state dynamic exchange process where the conformational flipping rates are equal to 220 sec^{-1} and 40 sec^{-1} for the fully protonated (pH 5.8) and deprotonated (pH 8.4) transporter, respectively. Although the rates were obtained in the absence of the membrane potential and could be further influenced within the cell membrane of the organism, the reduced exchange rate of the deprotonated state is in qualitative agreement with the coupling rules proposed for ion-coupled antiport[21].

Validation of Conformational Equilibrium in ΔpH Liposomes

Based on the difference in rate constants in the protonated and deprotonated states of EmrE, we predicted that the presence of a pH gradient (ΔpH) across a lipid bilayer and centered around the pKa of Glu-14 would bias EmrE's open conformation toward the higher pH side of the membrane. To test this hypothesis, we designed a tryptophan fluorescence assay in liposomes encompassing a ΔpH across the bilayer. Since the fluorescence emission profile of tryptophan is sensitive to the protonation state of Glu-14 (deprotonated - high fluorescence, protonated - low fluorescence)[13], the spectrum was used to determine the preferred orientation of inward- or outward-facing EmrE. Spectra were recorded for wild-type EmrE in four samples possessing the following pH^{in}/pH^{out} combinations: (1) 8.7/6.2, (2) 6.2/8.7, (3) 6.2/6.2, and (4) 8.7/8.7. The fluorescence signatures for the ΔpH vesicles are shown in Figure 2e and were found to be intermediate with respect to control vesicles having the same pH on both sides of the membrane. Since protonation and deprotonation are expected to occur faster than the conformational change[13], the relative signal intensities were used to estimate that ~83% of EmrE dimers were oriented in an open conformation toward the basic pH side of the bilayer in agreement with the rates measured from NMR. Note that disrupting the pH gradient caused the fluorescence spectra to look similar to the respective high and low pH controls, which confirmed the conformational preference in the asymmetric vesicles (Figure 2f). Similar results were also obtained in *E. coli* lipid vesicles (Supplementary Figure 6) and therefore support the conclusion that a pH gradient can influence the conformational equilibrium of a transporter in a native-like lipid composition.

Long-Range Allosteric Communication in EmrE

Why does protonation of Glu-14 impact the exchange kinetics? To delve into the mechanism, we mapped the Ile chemical shift perturbations between the Glu-14 protonated and deprotonated forms onto the X-ray structure of EmrE bound to tetraphenylphosphonium (TPP^+)[7]. Note that due to the resolution of the structure (3.8 Å, C_α model), the Ile methyl group chemical shift changes were plotted at the alpha carbon positions. Perturbations were observed in all TM domains of the transporter, including loop-2 connecting TM-2 with TM-3, as well as significant changes within TM-4 that is involved in dimer stability (Figure

3a)[7,22,23]. These changes persisted up to ~25 Å from the substrate binding pocket containing Glu-14 and were indicative of a long-range allosteric effect. Interestingly, chemical shift perturbation mapping for E14D showed dramatically attenuated changes for the mutant compared with the wild-type protein (Figure 3b), which suggested that the shorter side chain partially disrupted the allosteric communication within the transporter. A surprising finding for wild-type EmrE was that the perturbations to loop-2 adjoining TM2 and TM3 were different on one side of the transporter than the other. For example, the peaks corresponding to Ile-54 and Ile-62 within the inward-open face became very weak and disappeared upon protonation of Glu-14, while these same residues on the other monomer showed large chemical shift changes without significant intensity reductions (Supplementary Figure 7). These asymmetric perturbations combined with analysis of the EmrE crystal structure support a *latching model* of loop-2 to stabilize the open configuration of the transporter by excluding the N-terminal side of TM1 from the substrate-binding chamber (Figure 3c, Supplementary Figure 8). We propose that Glu-14 protonation leads to the disruption of these contacts resulting in large chemical shift perturbations and the observed conformational broadening in loop-2.

To further investigate the mechanistic features of loop-2, we engineered mutants at residue 54 (I54G and I54L) and performed resistance assays in *E. coli*. Interestingly, I54G completely abolished the resistance toward ethidium, but the I54L mutation gave no loss-of-function beyond that of wild-type EmrE (Figure 3d). The former is consistent with literature reports that I54C EmrE was a partial loss-of-function mutant[23,24]. Taken together with homology modeling showing the conservation of residue 54 as a large and hydrophobic amino acid residue (isoleucine, leucine, valine, or methionine)[25], these findings strongly implicate Ile-54 as an important site in loop-2.

EmrE Heterodimers to Probe Asymmetry of Loop-2

In the process of assigning Ile-54 in the methyl HMQC spectrum, we serendipitously discovered that I54L did not show peak doubling as observed for wild-type EmrE (Supplementary Figure 9). While this mutant did not disrupt the ability to confer drug resistance (Figure 3d), we surmised it might be useful for giving insight into the asymmetry of loop-2. As anticipated from the resistance assay, I54L was able to bind drugs and gave two populations upon addition of TPP^+ similar to that of wild-type EmrE (Figure 4a, b). These results strongly imply that the conformational exchange for I54L in the absence of drug was increased relative to the wild-type protein. Based on these findings and the asymmetric behavior of Ile-54 in the wild-type pH titration, we predicted that a heterodimer mixing experiment might break the 50/50 population of the NMR resonances. We also anticipated that this experiment would give insight into which of the two I54L mutations in the asymmetric dimer had a more pronounced effect on the dynamics. The experiment was carried out by preparing a 2:1 sample of I54L (no ^{13}C incorporation) and wild-type EmrE ($^{13}C_{\delta}$-Ile methyl labeled) and recording the $^{1}H/^{13}C$ Ile methyl spectrum. Remarkably, we observed ~2-fold more intense signals from one set of monomer peaks than the other in both DMPC (Figure 4c) and *E. coli* bicelles (Supplementary Figure 10). The opposite isotopic labeling experiment where I54L was enriched and wild-type was unlabeled gave more intense signals for the other set of monomer resonances (Figure 4d). To further substantiate

the results for Ile-54, we also carried out a second mixed dimer experiment with I62L − the other residue in loop-2 that displayed heterogeneity during the pH titration. Consistent with our results for I54L, the mixed dimer of isotopically enriched I62L and unlabeled wild-type also showed a conformational bias toward the same set of monomer resonances as that for I54L (Supplementary Figure 11). Therefore, the ability to influence the ratio of the two populations underscores the asymmetric contacts stabilizing the EmrE structure. Furthermore, while I54L did not disrupt the phenotype, indicating it did not influence the rate-limiting step in the transport cycle, these results support a differential stabilizing role for loop-2 between the open and closed side of the transporter. Taken together with our previous finding showing a well-defined structure for the loop adjoining TM3 and TM4[26], these findings strongly implicate an active role for loops in the allosteric communication network and ion-coupled transport process.

DISCUSSION

The findings described in this article unveil mechanistic details governing active transport in the SMR family modulated by acid-base chemistry of a conserved anionic residue. At pH values above the apparent pKa of Glu-14, our dynamics measurements indicated significantly reduced conformational exchange relative to the protonated form, which is consistent with vectorial transport rules[21]. However, unlike these strict rules that encompass perfect coupling of pH gradients with drug efflux, we observed small but significant conformational dynamics in the proton-unloaded form, suggesting that a minor population of EmrE might possess an outward-open conformation facing the periplasm under equilibrium conditions. There are a couple of key observations where the pH gradient is solely responsible for transport (i.e., divalent cations[27]) that suggest non-zero exchange under our experimental conditions may have significance *in vivo*. The first is polyamine import observed in the W63G mutant of EmrE, which implies the presence of an outward-open facing conformation[28]. This finding also suggests that Trp-63 may play an important role in transmitting the allosteric communication and conformational changes we observed upon protonation at Glu-14. A second observable is that EmrE was found to sensitize *E. coli* to methyl viologen under alkaline growth conditions where $pH_{periplasm} > pH_{cytoplasm}$[27]. Similar to this observable, we carried out resistance assays on E14D and wild-type EmrE and found that the mutant conferred sensitivity toward methyl viologen at a pH of 7.0 (Supplementary Figure 12). The latter two observations of drug sensitivity support net drug import into the cytoplasm and imply an outward facing conformation that is consistent with predictions from the NMR dynamics measurements. Interestingly, drug import has also been observed in single-site mutants of SugE[29], which is a closely related protein to EmrE and a member of the SMR family. Future studies will aim to investigate the conformational dynamics under native growth conditions to determine the role of the membrane potential as well as to further probe the allosteric communication network responsible for conformational switching in the membrane.

ONLINE METHODS

Protein Expression and Purification

The expression and purification of EmrE was carried out as previously described[10]. Briefly, EmrE was expressed as a fusion construct with maltose-binding protein and purified using affinity and size exclusion chromatography in *n*-dodecyl-β-D-maltopyranoside (DDM, Anatrace). [ILV-$^{13}CH_3$, U-^{15}N, ^{2}H] labeled EmrE samples were expressed with addition of precursors at a concentration of 50 mg/L 2-ketobutyric acid-4-^{13}C,3,3-$^{2}H_2$ sodium salt hydrate 1 hour before induction for Ile methyl labeling. The wild-type pH titrations to measure the acid dissociation constants (pKa) utilized ^{2}H background labeling and protonation at the Ile methyl groups, while the E14D samples were carried out with protonated sites and ^{13}C enrichment at the side chains. Isotopic enrichment for oriented solid-state NMR was accomplished by growing bacteria in the presence of ^{15}N NH_4Cl.

NMR Sample Preparation

For solution NMR studies, [ILV-$^{13}CH_3$, U-^{15}N, ^{2}H] labeled EmrE in DDM back-exchanged to ^{1}H at the amide positions was reconstituted in 10% (w/v) dimyristoyl-*sn*-glycero-3-phosphocholine/dihexanoyl-*sn*-glycero-3-phosphocholine (DMPC/DHPC) bicelles (q=0.33) with the lipid chains having perdeuteration (14:0 PC D54 and 6:0 D22, Avanti Polar Lipids). Ile methyl resonance assignments were obtained with single-site mutants prepared with the single-site mutagenesis kit from Agilent (Ile to either Val or Leu). The final NMR samples for solution NMR contained 0.5 mM EmrE, 20 mM Na_2HPO_4, 20 mM NaCl, 50 mM DTT and 0.02% NaN_3.

Solution NMR Spectroscopy

The solution NMR samples prepared for pH titrations were made in a volume of 375 μL to account for negotiable sample loss during adjustment of the pH. The pH was monitored before and after the experiment and found to fluctuate by ±0.01. Solution NMR experiments were performed on an Agilent DD2 600 MHz spectrometer with an HCN 5 mm triple resonance z-axis PFG room temperature probe. For the pH titrations, $^{1}H/^{13}C$ SOFAST-HMQC experiments[12] were acquired at 15 °C and 25 °C using a spectral width for ^{1}H and ^{13}C was 12019.2 Hz (83.2 msec acquisition time) and 4000 Hz (27.5 msec, evolution time), respectively and a recycle delay of 1 sec. The complete pH titration curve was collected over ~1–2 days and residues showing significant chemical shift perturbations (^{1}H > 0.03 ppm and ^{13}C > 0.1 ppm) were globally fit using Eqn 1, where δ_{HA} and δ_{A-} are the chemical shifts for the protonated and deprotonated transporter, respectively, while δ is the observed chemical shift at the different pH values.

$$\delta = \frac{\delta_{HA} + \delta_{A-} 10^{pH-pKa}}{1 + 10^{pH-pKa}} \quad (1)$$

The chemical shift perturbation between protonated and deprotonated EmrE at Glu-14 (Δδ) in the ^{13}C ($\Delta\delta_C$) and ^{1}H ($\Delta\delta_H$) dimensions of the methyl spectra were calculated using a ^{13}C scaling factor of 0.184 with the equation below.

$$\Delta\delta = \sqrt{(0.184\Delta\delta_C)^2 + \Delta\delta_H^2} \quad (2)$$

Methyl T_{1zz} exchange spectra were acquired with a mixing time 300 ms and a recycle delay of 1 sec.

Solid-State NMR Spectroscopy

Oriented solid-state NMR experiments were carried out using [U-^{15}N] EmrE at a concentration of ~2 mM in 25% DMPC/DHPC (w/v) bicelles at 37 °C. The HEPES concentration was increased to 150 mM to maintain pH control during the experiment. $YbCl_3$ was added to a final concentration of 3 mM to induce alignment of the bilayer normal parallel with respect to the magnetic field. For all experiments, the pH was checked before and after the experiments and found to be within ± 0.05 units. The PUREX experiment[20] was acquired on an Agilent DD2 spectrometer operating at a ^{1}H frequency of 600 MHz. A tau value of 0.25 msec was used for both the modulated and reference datasets. The range of mixing time was varied from 0.125 to 800 msec depending on the sample exchange rate. Acquisition of select points in duplicate was used to generate the error. The modulated and reference spectra were acquired with 2048 scans and 512 scans, respectively, which was needed to normalize the signal to noise ratio. The PUREX curve for each pH point required ~4–6 days of experimental acquisition time. The two datasets were subtracted to obtain the difference spectrum, which gave only signal intensities due to the exchange cross-peaks. The integrated spectra were plotted with respect to their mixing time and fit to the following equation to calculate the exchange rate (k_{ex}):

$$I_{AB}(t) = k_1(1 - e^{-k_{ex}t}) + k_3 \quad (3)$$

k_1 and k_3 are scaling factors to compensate for the signal intensities between different samples and a y-axis offset, respectively. The data were fit to obtain k_{ex} with the rate constants reported as k values in the text (i.e., $k = k_{ex}/2$). The errors reported in these values reflect the fitted error at a 90% confidence interval. All ^{15}N spectra were referenced to 41.5 ppm with the use of $^{15}NH_4Cl$(s).

Preparation of ΔpH Vesicles

Reconstitutions into the asymmetric pH membranes was accomplished through *n*-decyl-β-D-maltoside (DM, Anatrace) detergent by reconstituting the protein at a given pH and pelleting of the vesicles by ultracentrifugation followed by a gentle resuspension to the desired pH on the external side of the liposomes. Wild-type EmrE was reconstituted in DMPC or *E. coli* polar lipid extract (Avanti Polar Lipids, Inc.) where the pH values inside/outside the vesicles were set as pH^{in}/pH^{out}: 6.2/6.2, 6.2/8.7, 8.7/6.2, and 8.7/8.7. The buffer condition was 50 mM sodium phosphate and 20 mM NaCl. After reconstitution the proteoliposomes were centrifuged for 1.5 hr at 130,000 ×g and resuspended in the same buffer as that in the interior of the vesicles. This cycle was done a total of two times to ensure control of the inside pH. Prior to collection of the fluorescence spectra, the proteoliposomes were diluted

30-fold with the external buffer. After collection of the ΔpH experiments, a small amount of stock DDM was added (final ratio of DDM/lipid = 1/50, mol/mol) to disturb the pH gradient. Since the volume outside the vesicles was greater than that inside, the pH of the interior changed to the external value.

Fluorescence Measurements in ΔpH Vesicles

EmrE in 5 mM n-decyl-β-D-maltopyranoside (DM, Anatrace) detergent was reconstituted to a final concentration of 0.5 μM into 175 μM DMPC vesicles. Steady-state fluorescence experiments were carried out with an excitation wavelength (λ_{ex}) of 280 nm and an emission wavelength (λ_{em}) range of 200–400 nm with excitation and emission bandwidths of 2 nm and 4 nm, respectively. The emission range was chosen to confirm that Rayleigh scattering for all the ΔpH vesicles were similar. All the vesicles were incubated for 5 min at 25 °C prior to data collection. The data was an average of 2 scans. Each individual experiment was repeated two or more times. The uncorrected fluorescence data were directly plotted against all samples carried out in the same dataset. To make the plots, the relative fluorescence value on the y-axis was normalized to 1.0; no other normalization was performed on the data.

Resistance Assays

The PMS119EH vector for the resistance assay was a gift from Prof. Raymond Turner (University of Calgary). The cells containing vector were grown at 37 °C in an LB medium up to an OD_{600}=1.0. The bacteria were spotted onto LB-agar plate supplemented with carbenicillin at a range of dilutions (10^0 to 10^6). LB media for the plates and ethidium bromide stock solutions were buffered with 10 mM MOPS. The vector with no ribosome-binding site was selected as a control for the assay. Ethidium bromide concentration was chosen based on MIC (minimum inhibitory concentration) test performed at a particular pH. The assays used a concentration of 240 μM ethidium bromide.

Supplementary Material

Refer to Web version on PubMed Central for supplementary material.

ACKNOWLEDGMENTS

This work was supported by NIH grant R01AI108889 and start-up funds from New York University (to N.J.T.). M.L. acknowledges support from a Margaret-Strauss Kramer Fellowship. The NMR data collected with a cryoprobe at NYU was supported by an NIH S10 grant (OD016343). Data collected at the New York Structural Biology Center was made possible by a grant from NYSTAR. The authors thank Prof. Raymond Turner at the University of Calgary for providing wild-type EmrE in the pMS119EH vector, Dr. Min-Kyu Cho for assistance of the initial NMR experiments, and Prof. Daniela Buccella at New York University for usage of the spectrofluorometer.

REFERENCES

1. Higgins CF. Nature. 2007; 446:749–757. [PubMed: 17429392]
2. Bay DC, Rommens KL, Turner RJ. Biochimica et biophysica acta. 2007
3. Rapp M, Seppala S, Granseth E, von Heijne G. Science. 2007; 315:1282–1284. [PubMed: 17255477]
4. Schuldiner, S. What Can a Living Fossil Tell Us About Evolution and Mechanism of Ion-Coupled Transporters: The Story of Small Multidrug Transporters. In: Kramer, RZC., editor. Membrane

Transport Mechanism, Vol. Springer Series in Biophysics 17. Berlin Heidelberg: Springer; 2014. p. 233-248.

5. Fleishman SJ, et al. Journal of Molecular Biology. 2006; 364:54–67. [PubMed: 17005200]
6. Ubarretxena-Belandia I, Baldwin JM, Schuldiner S, Tate CG. The EMBO journal. 2003; 22:6175–6181. [PubMed: 14633977]
7. Chen YJ, et al. Proceedings of the National Academy of Sciences of the United States of America. 2007; 104:18999–19004. [PubMed: 18024586]
8. Muth TR, Schuldiner S. The EMBO journal. 2000; 19:234–240. [PubMed: 10637227]
9. Cho MK, Gayen A, Banigan JR, Leninger M, Traaseth NJ. J Am Chem Soc. 2014; 136:8072–8080. [PubMed: 24856154]
10. Gayen A, Banigan JR, Traaseth NJ. Angew Chem Int Ed Engl. 2013; 52:10321–10324. [PubMed: 23939862]
11. Morrison EA, et al. Nature. 2012; 481:45–50. [PubMed: 22178925]
12. Schanda P, Brutscher B. Journal of the American Chemical Society. 2005; 127:8014–8015. [PubMed: 15926816]
13. Adam Y, Tayer N, Rotem D, Schreiber G, Schuldiner S. Proceedings of the National Academy of Sciences of the United States of America. 2007; 104:17989–17994. [PubMed: 17984053]
14. Yerushalmi H, Schuldiner S. The Journal of biological chemistry. 2000; 275:5264–5269. [PubMed: 10681497]
15. Wilks JC, Slonczewski JL. J Bacteriol. 2007; 189:5601–5607. [PubMed: 17545292]
16. Jardetzky O. Nature. 1966; 211:969–970. [PubMed: 5968307]
17. Wang J, et al. J Magn Reson. 2000; 144:162–167. [PubMed: 10783287]
18. Marassi FM, Opella SJ. J Magn Reson. 2000; 144:150–155. [PubMed: 10783285]
19. Dutta S, Morrison EA, Henzler-Wildman KA. Biophys J. 2014; 107:613–620. [PubMed: 25099800]
20. deAzevedo ER, Bonagamba TJ, Schmidt-Rohr K. J Magn Reson. 2000; 142:86–96. [PubMed: 10617438]
21. Jencks WP. Methods in Enzymology. 1989; 171:145–164. [PubMed: 2531833]
22. Poulsen BE, Rath A, Deber CM. J Biol Chem. 2009; 284:9870–9875. [PubMed: 19224913]
23. Amadi ST, Koteiche HA, Mishra S, McHaourab HS. J Biol Chem. 2010; 285:26710–26718. [PubMed: 20551331]
24. Mordoch SS, Granot D, Lebendiker M, Schuldiner S. J Biol Chem. 1999; 274:19480–19486. [PubMed: 10383465]
25. Brill S, Sade-Falk O, Elbaz-Alon Y, Schuldiner S. J Mol Biol. 2015; 427:468–477. [PubMed: 25479374]
26. Banigan JR, Gayen A, Cho MK, Traaseth NJ. J Biol Chem. 2015; 290:805–814. [PubMed: 25406320]
27. Rotem D, Schuldiner S. J Biol Chem. 2004; 279:48787–48793. [PubMed: 15371426]
28. Brill S, Falk OS, Schuldiner S. Proc Natl Acad Sci U S A. 2012; 109:16894–16899. [PubMed: 23035252]
29. Son MS, et al. Biochem Biophys Res Commun. 2003; 312:914–921. [PubMed: 14651958]

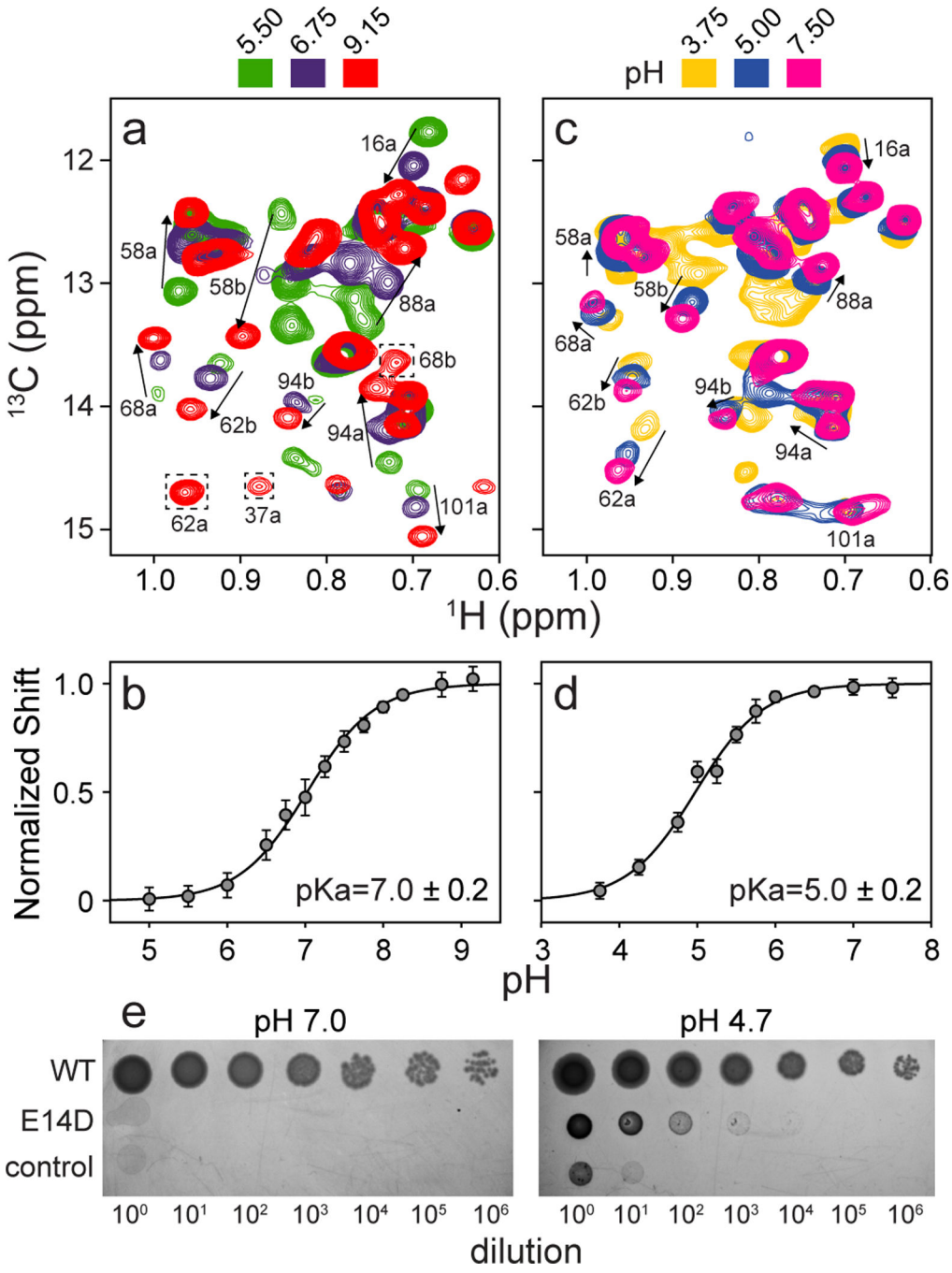

Figure 1. pH-induced conformational changes to EmrE

Overlay of ^{1}H/^{13}C SOFAST-HMQC NMR spectra for Ile methyl groups at the indicated pH values for (a) wild-type and (c) E14D EmrE. Arrows indicate the direction of chemical shift changes from low to high pH. (b, d) Normalized chemical shift perturbations at 25 °C for wild-type and E14D EmrE, respectively. The global fit to individual sites gave the indicated apparent pKa values of 7.0 and 5.0. The error bars reflect the standard deviation among residues used to construct the fit. (e) *E. coli* resistance assays using serial 10-fold dilutions in the presence of an LB agar plate with 240 μM ethidium bromide and carbenicillin. The

assays were performed at pH 7.0 and 4.7 using wild-type EmrE, E14D, and a control that contained no expressed EmrE. Control dilution experiments in the absence of ethidium are shown in Supplementary Figure 13. The resistance assay was repeated with similar results at least five times.

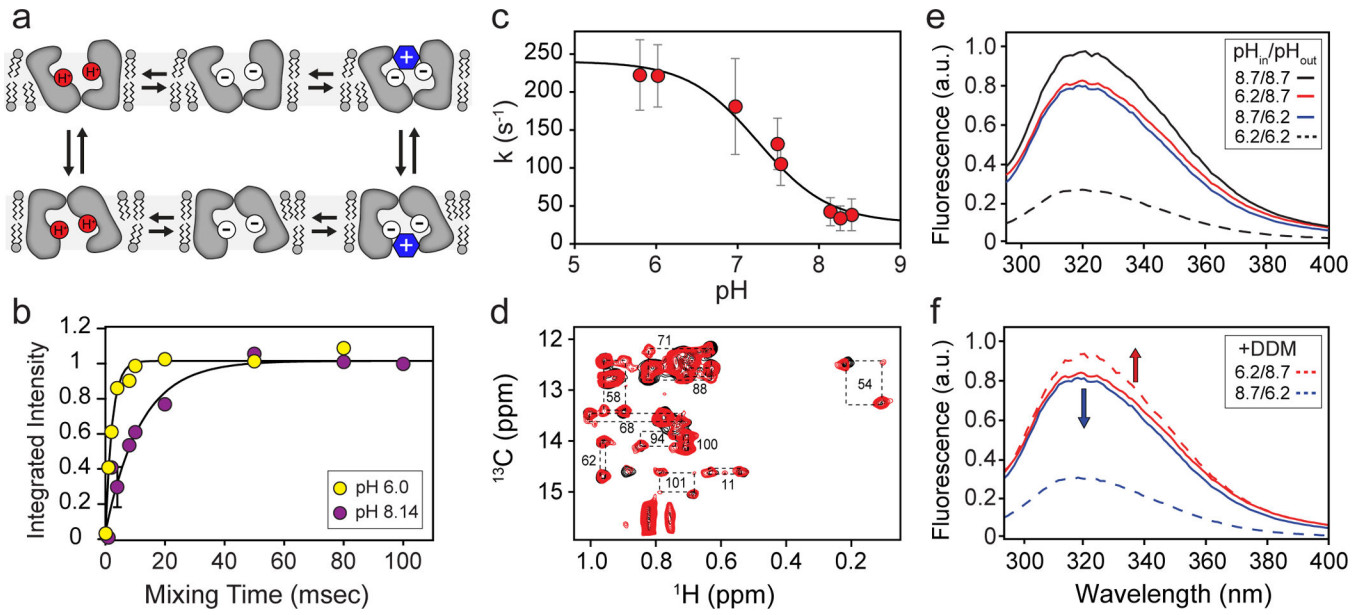

Figure 2. Glu-14 protonation sets the resting state

(a) Schematic of the alternating access model. The vectorial transport rules forbid conformational exchange in the fully unloaded transporter[21]. (b) Conformational exchange dynamics probed with PUREX in aligned bicelles at the two indicated pH values. (c) Quantified exchange rates as a function of pH (error bars reflect a 90% confidence interval). All of the PUREX curves used to construct panel c are shown in Supplementary Figure 5. (d) Overlay of a methyl T_{1zz} experiment (red) and HSQC spectrum (black) of deprotonated EmrE (pH 9.15). The dotted boxes connect the two exchanging peaks and suggest the presence of conformational dynamics in the Glu-14 deprotonated transporter. (e) Tryptophan fluorescence of EmrE in DMPC vesicles under different pH combinations. (f) Disruption of the ΔpH vesicles with addition of DDM detergent. The same fluorescence result was obtained in three independent trials.

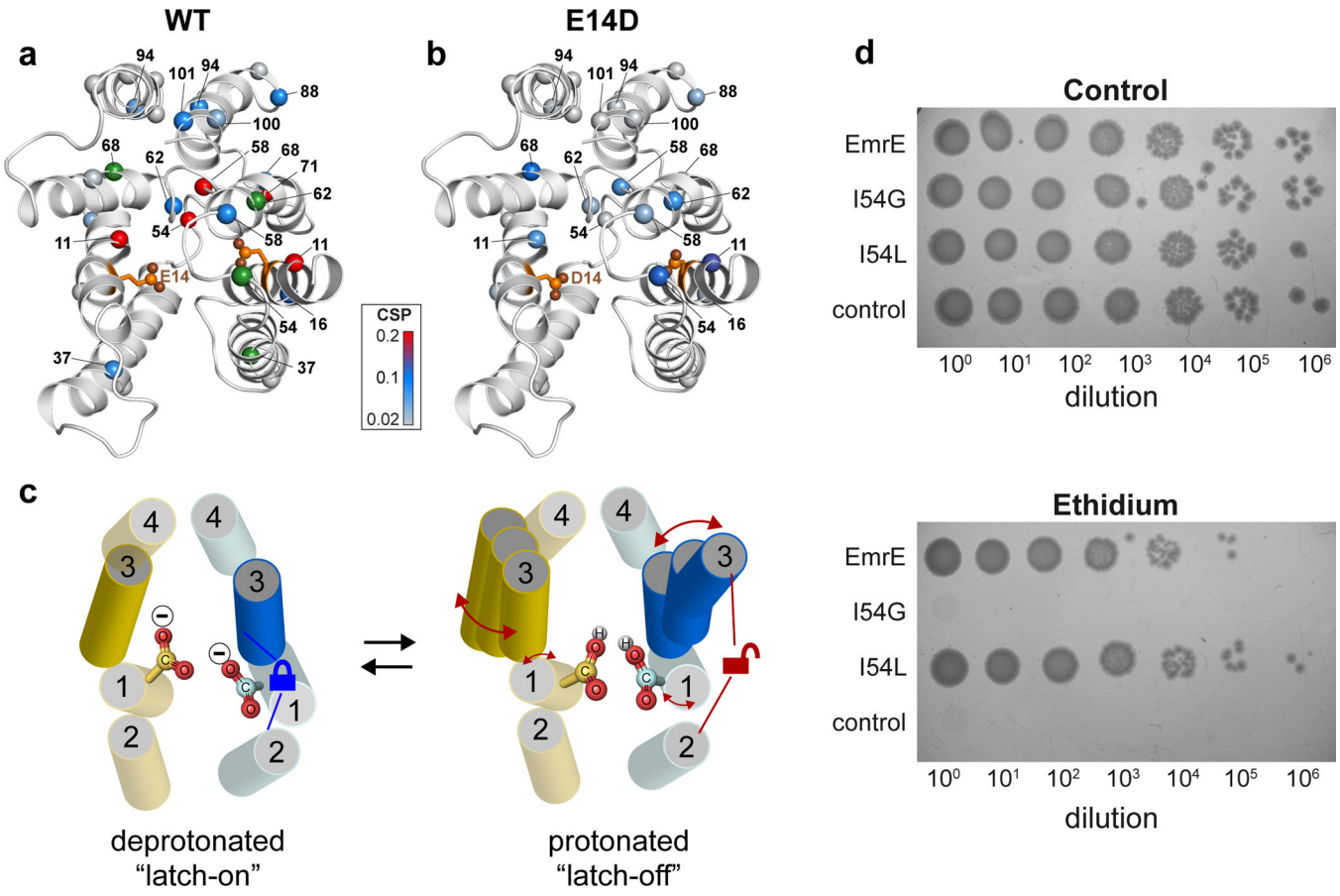

Figure 3. Allosteric conformational change from Glu-14 protonation

(a) Heat map of the chemical shift perturbations between pH=5.5 and pH=9.15 mapped onto the Cα atoms of EmrE (*3B5D*)[7]. Green spheres denote residues that became too weak to be followed in the pH titration below ~7.0. (b) Perturbation data for E14D EmrE mapped onto the same structure (difference between pH=3.75 and pH=7.5). Both perturbations datasets are viewed from the perspective of the open side of the transporter. (c) Cartoon model illustrating the proposed role of the latch in stabilizing the open conformation of EmrE, which is consistent with the NMR perturbations in the pH titration, analysis of the crystal structure of EmrE, and the loss of resistance for I54G. Note that the TM domains are indicated with numbers. (d) *E. coli* resistance assays carried out using serial 10-fold dilutions on an LB agar plate (pH=7) containing carbenicillin in the absence (top) and presence (bottom) of 240 μM ethidium bromide. The plasmid contained wild-type EmrE, I54G, I54L, or a control vector where EmrE was not expressed. The resistance assay was repeated twice with the same result.

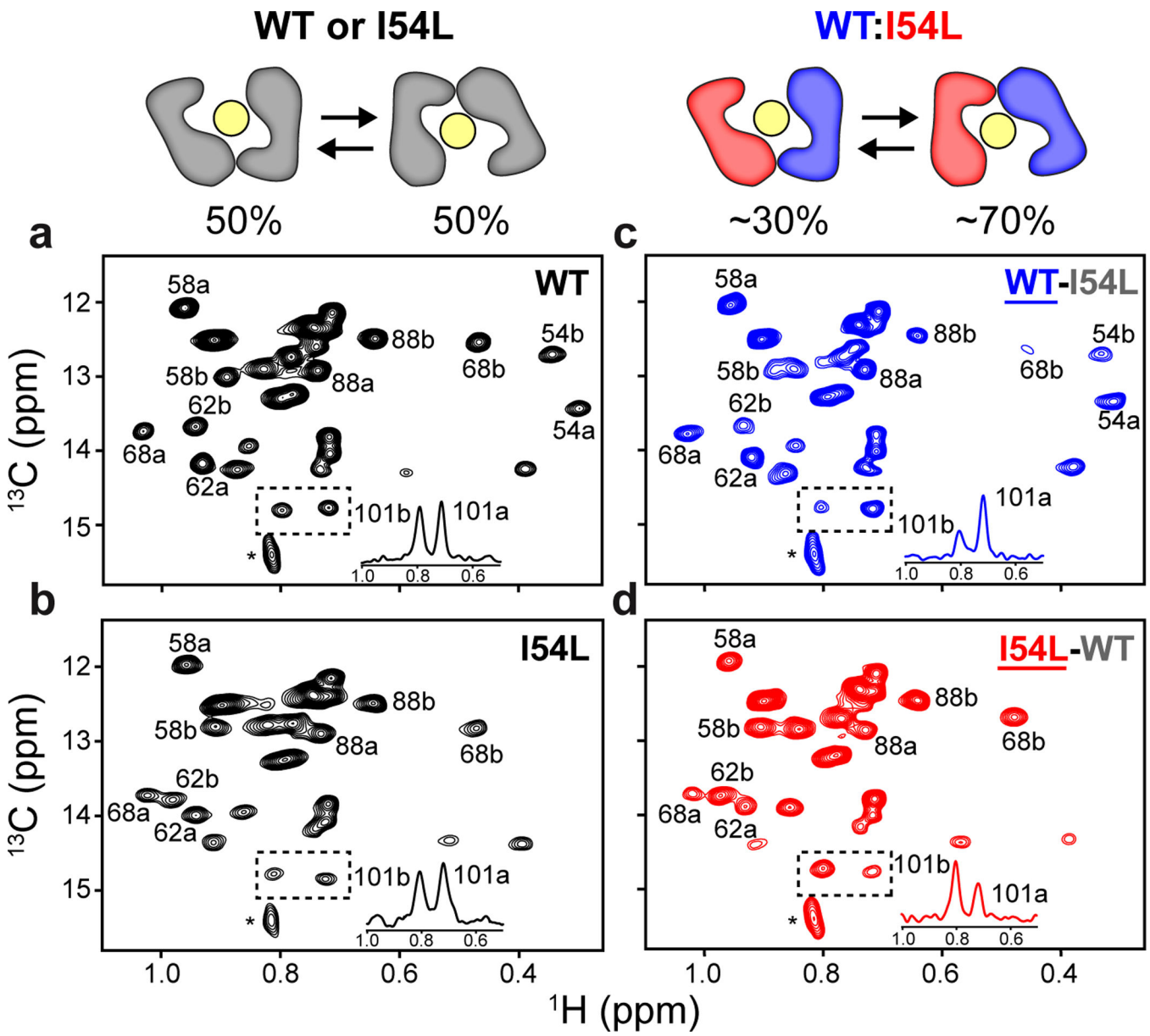

Figure 4. Conformational bias from loop-2 mutant in mixed EmrE dimers

^{1}H/^{13}C SOFAST-HMQC experiments of (a) wild-type and (b) I54L EmrE in the presence of TPP^{+}. (c and d) Mixed dimer of wild-type and I54L where the ^{13}C enriched protein is underlined. The mixed sample where I54L was NMR enriched gave more intense peaks for monomer “b” whereas the labeled wild-type gave greater peak intensities for monomer “a”. Insets within the HMQC spectra show 1D slices for Ile-101 to illustrate the skewed populations. The asterisks indicate lipid peaks.